

Lotus Desbiolles
Sebastian Leschka
André Plass
Hans Scheffel
Lars Husmann
Oliver Gaemperli
Elisabeth Garzoli
Borut Marincek
Philipp A. Kaufmann
Hatem Alkadhi

Evaluation of temporal windows for coronary artery bypass graft imaging with 64-slice CT

Received: 19 January 2007
Revised: 3 May 2007
Accepted: 11 May 2007
Published online: 17 July 2007
© Springer-Verlag 2007

L. Desbiolles · S. Leschka ·
H. Scheffel · L. Husmann · E. Garzoli ·
B. Marincek · H. Alkadhi (✉)
Institute of Diagnostic Radiology,
University Hospital Zurich,
Raemistrasse 100,
8091 Zurich, Switzerland
e-mail: hatem.alkadhi@usz.ch
Tel.: +41-1-2553662
Fax: +41-1-2554443

A. Plass
Clinic for Cardiovascular Surgery,
University Hospital Zurich,
Zurich, Switzerland

O. Gaemperli · P. A. Kaufmann
Cardiovascular Center,
University Hospital Zurich,
Zurich, Switzerland

P. A. Kaufmann
Center for Integrative Human
Physiology, University of Zurich,
Zurich, Switzerland

Abstract Temporal windows providing the best image quality of different segments and types of coronary artery bypass grafts (CABGs) with 64-slice computed tomography (CT) were evaluated in an experimental set-up. Sixty-four-slice CT with a rotation time of 330 ms was performed in 25 patients (four female; mean age 59.9 years). A total of 84 CABGs (62 individual and 22 sequential grafts) were evaluated, including 28 internal mammary artery (33.3%), one radial artery with sequential grafting (2.4%), and 54 saphenous vein grafts (64.3%). Ten data sets were reconstructed in 10% increments of the RR-interval. Each graft was separated into segments (proximal and distal anastomosis, and body), and CABG types were grouped according to target arteries. Two readers independently assessed image quality of each CABG segment in each temporal window. Diagnostic image quality was found with good inter-observer agreement ($\kappa=0.62$) in 98.5% (202/205)

of all graft segments. Image quality was significantly better for saphenous vein grafts versus arterial grafts ($P<0.001$) and for distal anastomosis to the right coronary compared with other target coronary arteries ($P<0.05$). Overall, best image quality was found at 60%. Image quality of proximal segments did not significantly vary with the temporal window, whereas for all other segments image quality was significantly better at 60% compared with other temporal windows ($P<0.05$). Sixty-four-slice CT provides best image quality of various segments and types of CABG at 60% of the RR-interval.

Keywords 64-slice computed tomography · Coronary artery bypass graft · Temporal window

Introduction

Invasive coronary angiography (ICA) currently is considered the reference standard for evaluation of coronary artery bypass graft (CABG) patency. However, the small but inevitable rate of procedure-related complications, the cost extensiveness, and patient discomfort with ICA have motivated the exploration of other non-invasive means for CABG surveillance.

Several multidetector-row computed tomography (MDCT) angiography studies have demonstrated a high diagnostic accuracy for the assessment of CABG patency [1–5];

however, visualization of up to 22% of CABGs was hampered by artifacts and segments were considered non-evaluative [6, 7]. Artifacts occurring with CT angiography of CABG usually derive from surgical clips and cardiac motion [2]. Thereby, the distal anastomosis of a CABG is commonly more prone to motion artifacts because of its close proximity to the rapidly moving coronary arteries. To compensate for motion artifacts, images are usually reconstructed at different phases of the cardiac cycle to identify the time-point with lowest vessel motion and minimal motion artifacts.

Compared with previous CT scanners, 64-slice CT provides a higher temporal resolution of 165 ms in combination with a maximum spatial resolution of $0.4 \times 0.4 \times 0.4 \text{ mm}^3$ [8], that possibly allows CABG imaging at a more narrow temporal window and consequently would reduce the amount of reconstructed data to be handled [9]. Electrocardiogram (ECG) pulsing has been advocated for radiation dose reduction; however, its implementation requires that visualization of all bypass segments, and particularly the distal anastomosis and the native coronary arteries, succeeds with at least diagnostic image quality in a narrow temporal window in diastole. Initial CABG studies with 64-slice CT have reconstructed data at 40–70% of the R-R interval [4] or at various time intervals throughout the cardiac cycle [10]; however, these studies were aimed at the assessment of CABG patency rather than for systematic assessment of the relationship of image quality to temporal windows for CABG imaging. Thus, the purpose of this study was to evaluate the temporal windows providing best image quality for different segments and various types of CABG, and particularly the distal anastomosis, with 64-slice CT.

Materials and methods

Patients and grafts

Between April 2005 and June 2005, 37 consecutive patients (28 male, nine female; mean age 61.8 years; range 37–77 years) underwent CABG in our hospital and were asked to take part in a CT image quality study for CABG imaging. All CT scans were performed for experimental purposes only. Exclusion criteria for CT were allergy to iodinated contrast medium ($n=4$) and renal

insufficiency (creatinine level $>120 \mu\text{mol/l}$; $n=3$). Five patients refused to take part in the study. Thus, the final study population consisted of 25 patients (21 male, four female; mean age 59.9 years; range 37–77 years) harbouring 84 CABG. All CT examinations were performed in the early post-operative period, with the mean time interval between CABG surgery and CT examination being 7 days (range 3–13 days). All CT examinations were performed for study purpose only. Four (16%) patients had prosthetic valves (aortic valve, $n=3$; mitral valve, $n=1$), and two (8%) patients had pacemakers. Twenty-one patients (84%) received oral beta-blockers as part of their baseline medication, no additional beta-blockers were given prior to CT in order to evaluate optimal temporal windows in an experimental setup with a variety of heart rates to test for the strength of 64-slice CT in providing diagnostic image quality. The study was approved by the local ethics committee and all patients gave written informed consent.

Figure 1 demonstrates the distribution of the different CABGs. According to a previous study [11], grafts were classified according to the site of the distal graft anastomosis into three types: type 1 grafts are connected to the left anterior descending artery, its side branches, or an intermediate artery if present; type 2 grafts had distal anastomosis to the left circumflex artery; type 3 grafts had distal anastomosis to the right coronary artery. The coronary artery tree was subdivided into 15 segments according to the guidelines of the American Heart Association [12].

CT data acquisition and image reconstruction

For all scans, a CT scanning protocol was used primarily designed for the experimental set-up of this study. All scans

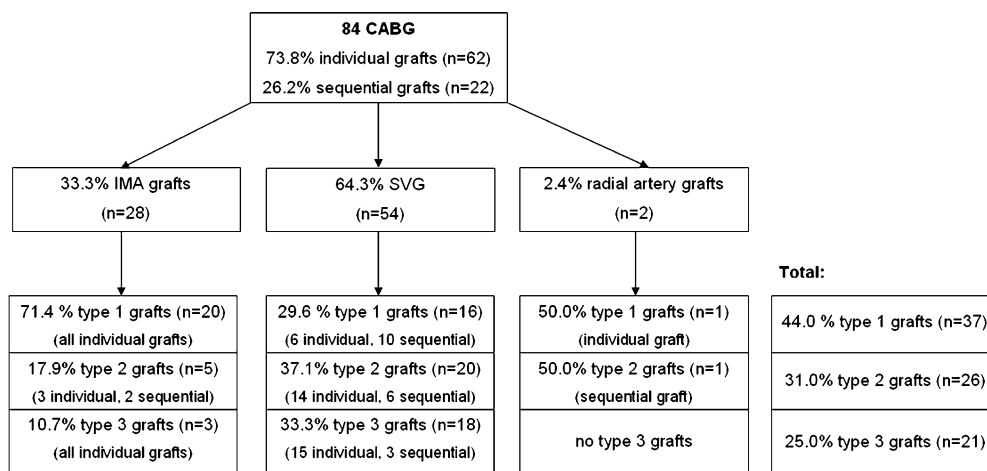


Fig. 1 Flow chart showing the distribution of the different CABGs in internal mammary artery (IMA) grafts, saphenous vein grafts (SVG), and radial artery grafts. According to a previous study [11], grafts were classified according to the site of the distal graft anastomosis into three types: type 1 grafts are connected to the left

anterior descending artery, its side branches, or an intermediate artery if present; type 2 grafts had distal anastomosis to the left circumflex artery; type 3 grafts had distal anastomosis to the right coronary artery. Two patients had a Y-graft configuration with the SVG dividing into two separate grafts near the proximal anastomosis

were performed using a 64-slice CT scanner (Somatom Sensation 64, Siemens Medical Solutions, Forchheim, Germany) with the following parameters: detector collimation 32×0.6 mm, slice collimation 64×0.6 mm, gantry rotation time 330 ms, pitch 0.2, tube potential 120 kV, and tube current time product 650 mAs. A bolus of 90 ml of iodixanol (Visipaque 320, 320 mg/ml; GE Healthcare, Buckinghamshire, UK) followed by 30 ml saline solution was continuously injected into a right antecubital vein via a 18-gauge catheter at a flow rate of 5 ml/s. Bolus tracking was performed with a region of interest (ROI) placed into the ascending aorta, and image acquisition in a cranio-caudal direction was automatically started 5 s after the signal attenuation reached a predefined threshold of 120 Hounsfield units (HU). The scanning range was planned individually for each patient and included the entire course of the venous graft but did not extend to the origin or proximal part of the internal mammary artery grafts, in order to maintain a manageable breath-hold period and to not further increase radiation exposure. The mean cranio-caudal distance of the acquired volume was 17.2 cm (range, 16–19 cm). All imaging was performed in inspiratory breath-hold. ECG pulsing was not used in this study in order not to affect image quality evaluation in systole by increased image noise.

Synchronized to the ECG, CT data sets were retrospectively reconstructed throughout the cardiac cycle in 10% steps from 0% to 90% of the R-R interval with a slice thickness of 1 mm (increment 0.8 mm) using a medium soft-tissue convolution kernel (B30f). The field of view was manually adjusted to encompass the heart including the grafts. The adaptive cardio volume approach was used which automatically reconstruct the scan data synchronized to the ECG by a single sector (≤ 62 bpm) or two sector algorithm (> 62 bpm) using data from one or two consecutive heartbeats [7]. All reconstructed image datasets were anonymized with regards to the percentage of the temporal window, were coded and arranged in random order, and were transferred to an external workstation (Leonardo, Siemens) for analysis.

CT data analysis

Two experienced and blinded cardiovascular radiologists independently evaluated the CT data for image quality in CABG segments. Optimal window settings were individually adjusted for assessment of CABG in each patient. Multiplanar reformations were used for image quality assessment. Each saphenous vein grafts and the one radial artery graft were divided into three segments: a proximal anastomosis, graft body, and distal anastomosis; internal mammary artery graft was divided into graft body and distal anastomosis. In case of a Y graft configuration, the proximal part of the common bypass and the two secondary bypasses were evaluated individually. Sequential grafts

were divided into graft body and distal anastomosis. All graft segments were separately evaluated in all ten data sets regarding image quality using previously published modified five-point Likert grading scales [8, 13] (Table 1). A score of 3–5 was considered acceptable in terms of clinical diagnostics.

Statistical analysis

Statistical analysis was performed using commercially available software (SPSS 12.0, Chicago, USA). Data were expressed as mean \pm standard deviation for continuous variables and as frequencies and percentages for categorical variables. Inter-observer agreements were assessed by using kappa values and interpreted as follows: a kappa of 0.80 and higher was considered as excellent agreement, between 0.40 and 0.80 as moderate to substantial, between 0.20 and 0.40 as fair, and less or equal to 0.20 as slight or poor agreement. Multivariate calculations with repeated measures analysis of variance (ANOVA) was performed to compare image quality in different temporal windows. Subanalysis was performed for each segment between arterial (e.g. internal mammary artery and radial artery grafts) and saphenous vein grafts, between individual and sequential grafts, and the three type of grafts according to the target coronary artery. The Wilcoxon signed-rank test was used for pair-wise comparison of mean image quality at the individual optimal temporal window of arterial versus venous bypass grafts, in different graft types, and individual versus sequential graft segments. The Wilcoxon signed-rank test was also performed to test for image quality differences of each CABG segment, depending on a

Table 1 Definition of image quality score [11]

Score	Bypass graft segments
Excellent (score 5)	No motion artifacts with clear delineation of the entire segment
Good (score 4)	Minor motion artifacts seen as a discrete tail or streak with slight blurring of the segment, no stair step artifacts; image quality not affected by metallic clips
Moderate (score 3)	Broader motion artifacts extending less than 5mm from the vessel center, with moderate blurring of the segment; stair step artifacts of $< 25\%$ of vascular diameter; metallic clips degrade image quality but not hinders vessel wall/lumen assessment
Poor (score 2)	Severe motion artifacts with doubling and/or blurring of the segment; poor attenuation or metal clips hinder vessel assessment
Not-evaluative (score 1)	Non-opacified or non-visible graft segment

single- or a two-sector reconstruction. A *P* value of <0.05 indicated a statistically significant difference.

Results

The imaging protocol was well tolerated by all patients, and all were able to hold their breath during CT data acquisition. All patients had a sinus rhythm during scanning. Mean heart rate was 74.2 ± 13.0 beats per minute (bpm) (range 50–95 bpm). In 14 patients (56%) the heart rate was ≤ 62 bpm and images were reconstructed by a one-sector algorithm, while in 11 patients (44%) heart rate was >62 bpm and images were reconstructed by a two-sector algorithm.

Overall image quality of CABG

In total, 205 CABG segments (35 proximal anastomoses, 63 individual graft bodies, 23 sequential graft bodies, and 84 distal anastomoses) were analysed. Table 2 summarizes the image quality scores of all CABG segments using the individual best temporal window. Diagnostic image quality (i.e., scores 3–5) was achieved in 98.5% (202/205) of all CABG segments. Overall image quality in all CABG segments was 4.09 ± 0.73 for reader 1 and 3.95 ± 0.67 for reader 2, with a good inter-observer agreement ($\kappa=0.62$). Image quality of the graft bodies of one radial artery including its sequential graft and one left internal mammary artery graft were considered poor (score 2) in any phase of the cardiac cycle, due to presence of metallic clips. However, all distal anastomoses of these two grafts were rated as being of diagnostic quality.

Overall image quality and optimal temporal window depending on arterial or venous graft

The mean image quality of all CABG segments, graft bodies and distal anastomosis were significantly better for SVG than for arterial graft segments (all $P < 0.001$; Fig. 2; Table 3). There was no significant difference in image

Table 2 Overall image quality scores of all bypass graft segments for both readers in the individual best temporal window

	Mean image quality scores in all bypass graft segments	
	Reader 1	Reader 2
Excellent (score 5)	50.7% (104/205)	43.0% (88/205)
Good (score 4)	32.7% (67/205)	34.1% (70/205)
Moderate (score 3)	14.6% (31/205)	21.4% (44/205)
Poor (score 2)	1.4% (3/205)	1.4% (3/205)
Not evaluative (score 1)	—	—

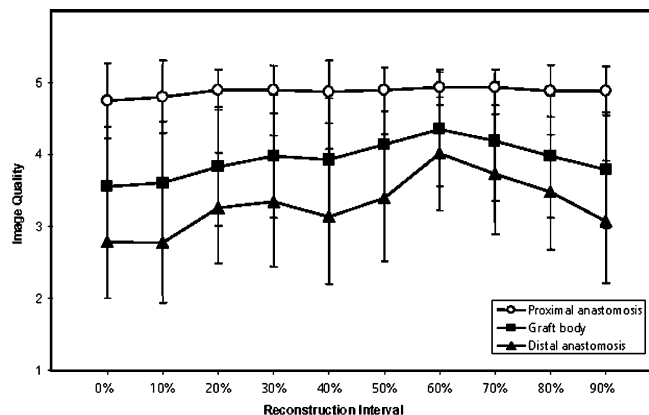


Fig. 2 Graph demonstrating the mean image quality of (1) proximal anastomosis, (2) graft body, and (3) distal anastomosis of all graft types as assessed by both readers on 64-slice CT angiograms. Error bars indicate \pm SD. Image quality was not significantly different for various temporal windows in proximal anastomosis and body segments (both *P* values not significant), but image quality was significantly better at a 60% temporal windows compared with other temporal windows for the visualization of distal anastomosis ($P < 0.001$)

quality of any CABG segment in relation to the reconstruction algorithm used (*P* value not significant; Table 4).

Image quality of proximal anastomoses of the SVG and for graft body segments of arterial and venous grafts did not significantly differ between the temporal windows (*P* value not significant; Table 5; Fig. 3). For distal anastomoses image quality at 60% of the R-R interval for both arterial and saphenous vein graft was significantly better compared with the other temporal windows ($P < 0.001$; Table 5; Fig. 4).

Overall image quality and optimal temporal window depending on target artery

Image quality for type 3 grafts was significantly better compared with type 1 ($P < 0.05$) and type 2 grafts ($P < 0.05$). There was no significant difference in image quality of the distal anastomosis between type 1 and type 2 grafts (*P* value not significant; Table 3).

Image quality of the distal anastomoses at right coronary artery, left anterior descending artery, and left circumflex artery was significantly better at a temporal window of 60% of the cardiac cycle compared with all other temporal windows ($P < 0.05$; $P < 0.02$; and $P < 0.002$, respectively; Fig. 5).

Overall image quality and optimal temporal window depending on individual or sequential graft

There was no significant difference in image quality between individual and sequential graft bodies and distal anastomosis (both *P* values not significant; Table 3).

Table 3 Comparison of mean image quality depending on arterial or venous bypass graft segments, for distal anastomosis depending on the target coronary artery, and individual versus sequential bypass graft segments. (Data are mean image quality \pm SD; *SVG* saphenous vein graft, *n.s.* not significant)

	Reader 1	Reader 2	Kappa	<i>P</i> value ^a
Image quality depending on arterial or venous bypass graft segments				
All arterial graft segments	3.28 \pm 0.84	3.01 \pm 0.84	0.76	<0.001
All SVG segments	3.92 \pm 0.81	3.72 \pm 0.74	0.70	
Proximal anastomosis (SVG)	4.87 \pm 0.39	4.88 \pm 0.32	0.90	—
Graft bodies (arterial grafts)	3.33 \pm 0.79	3.20 \pm 0.79	0.82	<0.001
Graft bodies (SVG)	4.37 \pm 0.72	4.17 \pm 0.68	0.62	
Distal anastomosis (arterial grafts)	3.22 \pm 0.89	2.83 \pm 0.89	0.70	<0.001
Distal anastomosis (SVG)	3.47 \pm 0.90	3.27 \pm 0.80	0.69	
Image quality depending on the target coronary artery^b				
Type 1	3.34 \pm 0.70	3.09 \pm 0.71	0.58	<0.05 ^c
Type 2	3.09 \pm 0.77	2.81 \pm 0.64	0.68	<0.05 ^c
Type 3	3.93 \pm 0.81	3.69 \pm 0.81	0.71	—
Image quality depending on individual or sequential graft segments				
Graft body (individual graft)	4.48 \pm 0.67	4.23 \pm 0.69	0.76	<i>n.s.</i>
Graft body (sequential graft)	4.17 \pm 0.77	3.96 \pm 0.68	0.70	
Distal anastomosis (individual graft)	3.52 \pm 0.87	3.19 \pm 0.81	0.51	<i>n.s.</i>
Distal anastomosis (sequential graft)	3.38 \pm 0.70	3.20 \pm 0.63	0.81	

^a*P* values are calculated for both readers separately (Wilcoxon signed-rank test)

^bGrafts were classified according to the site of the distal graft anastomosis into three types [11]: type 1 grafts are connected to the left anterior descending artery, its side branches, or an intermediate artery if present; type 2 grafts had distal anastomosis to the left circumflex artery; type 3 grafts had distal anastomosis to the right coronary artery

^c*P* value accounts for pair-wise comparison to image quality in type 3 grafts (Wilcoxon signed-rank test). No significant difference was present between image quality of distal anastomosis in type 1 and type 2 grafts

Image quality at 60% of the R-R interval for both individual and sequential graft bodies and distal anastomosis, respectively, was significantly better compared with the other temporal windows (both *P* values <0.001; Table 5; Fig. 6).

Discussion

Our study demonstrates that 64-slice CT angiography provides diagnostic image quality for all venous and 95%

of all arterial CABG segments. It allows complete visualization of all distal anastomoses irrespective of the graft type. Mean image quality was better in SVG compared with arterial grafts for both body segments and distal anastomosis, and was better in distal CABG anastomoses to the right coronary artery compared with the left anterior descending artery and left circumflex artery. There was no significant difference in visualization of individual versus sequential grafts. Image quality of proximal anastomoses and graft body did not depend on the temporal window during the cardiac cycle, whereas the 60% reconstruction

Table 4 Comparison of mean image quality of different graft segments depending on image reconstruction by a single-sector (\leq 62 bpm) or a two-sector algorithm ($>$ 62 bpm) [7]. (Data are mean image quality \pm SD; *SVG* saphenous vein graft, *n.s.* not significant)

	Single sector reconstruction (<i>n</i> =14)	Two sector reconstruction (<i>n</i> =11)	<i>P</i> value ^a
All arterial graft segments	3.14 \pm 0.87	3.15 \pm 0.67	<i>n.s.</i>
All SVG segments	3.82 \pm 0.80	3.89 \pm 0.77	<i>n.s.</i>
Proximal anastomosis (SVG)	4.96 \pm 0.38	4.85 \pm 0.54	<i>n.s.</i>
Graft bodies (arterial grafts)	3.39 \pm 0.61	3.31 \pm 0.59	<i>n.s.</i>
Graft bodies (SVG)	4.26 \pm 0.89	4.27 \pm 0.60	<i>n.s.</i>
Distal anastomosis (arterial grafts)	3.10 \pm 0.76	3.00 \pm 0.76	<i>n.s.</i>
Distal anastomosis (SVG)	3.35 \pm 0.78	3.37 \pm 0.89	<i>n.s.</i>

^a*P* values are calculated for the mean image quality of the individual bypass segment depending on the reconstruction algorithm used (Wilcoxon signed-rank test)

Table 5 Mean image quality of the different type and segment of graft as assessed by both readers (R1 and R2) at ten temporal windows within the cardiac cycle. (Data are mean image quality \pm SD)

Type of graft/graft Segment	0%	10%	20%	30%	40%	50%	60%	70%	80%	90%	Kappa
All graft types											
Body of graft (R1)	3.67 \pm 0.94	3.73 \pm 0.94	3.98 \pm 0.90	4.04 \pm 0.91	3.99 \pm 0.88	4.19 \pm 0.88	4.38 \pm 0.84	4.21 \pm 0.88	4.10 \pm 0.92	3.90 \pm 0.90	0.70
Body of graft (R2)	3.36 \pm 0.85	3.49 \pm 0.89	3.68 \pm 0.89	3.96 \pm 0.88	3.90 \pm 0.88	3.96 \pm 0.86	4.34 \pm 0.81	4.13 \pm 0.86	3.81 \pm 0.90	3.63 \pm 0.82	
Distal anastomosis (R1)	2.90 \pm 0.87	2.85 \pm 0.89	3.37 \pm 0.86	3.43 \pm 0.96	3.20 \pm 0.96	3.54 \pm 0.97	4.16 \pm 0.83	3.81 \pm 0.94	3.58 \pm 0.87	3.18 \pm 0.90	0.70
Distal anastomosis (R2)	2.62 \pm 0.77	2.69 \pm 0.80	3.09 \pm 0.79	3.26 \pm 0.87	3.05 \pm 0.89	3.25 \pm 0.84	3.86 \pm 0.78	3.60 \pm 0.79	3.31 \pm 0.79	2.92 \pm 0.85	
Arterial graft											
Body of graft (R1)	3.00 \pm 0.65	3.11 \pm 0.75	3.33 \pm 0.73	3.37 \pm 0.74	3.41 \pm 0.74	3.48 \pm 0.93	3.70 \pm 0.91	3.50 \pm 0.88	3.33 \pm 0.91	3.12 \pm 0.74	0.82
Body of graft (R2)	2.76 \pm 0.72	2.93 \pm 0.71	3.00 \pm 0.81	3.32 \pm 0.77	3.32 \pm 0.81	3.29 \pm 0.93	3.68 \pm 0.81	3.52 \pm 0.87	3.16 \pm 0.89	3.00 \pm 0.64	
Distal anastomosis (R1)	2.73 \pm 0.82	2.76 \pm 0.87	3.31 \pm 0.89	3.28 \pm 0.96	3.10 \pm 0.93	3.28 \pm 0.97	3.93 \pm 0.79	3.54 \pm 0.81	3.35 \pm 0.89	3.00 \pm 0.98	0.70
Distal anastomosis (R2)	2.14 \pm 0.97	2.50 \pm 0.79	2.86 \pm 0.97	3.14 \pm 0.93	2.93 \pm 0.85	2.96 \pm 0.79	3.71 \pm 0.71	3.00 \pm 0.98	2.64 \pm 0.97	2.43 \pm 0.95	
Venous graft											
Proximal anastomosis (R1)	4.74 \pm 0.57	4.79 \pm 0.53	4.91 \pm 0.28	4.88 \pm 0.40	4.88 \pm 0.40	4.85 \pm 0.43	4.94 \pm 0.23	4.94 \pm 0.25	4.87 \pm 0.42	4.90 \pm 0.57	0.80
Proximal anastomosis (R2)	4.73 \pm 0.52	4.82 \pm 0.46	4.88 \pm 0.33	4.91 \pm 0.29	4.88 \pm 0.41	4.91 \pm 0.29	4.94 \pm 0.24	4.93 \pm 0.25	4.90 \pm 0.30	4.87 \pm 0.34	
Body of graft (R1)	4.00 \pm 0.89	4.07 \pm 0.88	4.33 \pm 0.80	4.41 \pm 0.79	4.30 \pm 0.79	4.56 \pm 0.60	4.76 \pm 0.51	4.56 \pm 0.64	4.48 \pm 0.65	4.29 \pm 0.71	0.42
Body of graft (R2)	3.69 \pm 0.73	3.80 \pm 0.77	4.06 \pm 0.70	4.31 \pm 0.73	4.22 \pm 0.75	4.33 \pm 0.55	4.71 \pm 0.54	4.47 \pm 0.66	4.18 \pm 0.68	3.98 \pm 0.69	
Distal anastomosis (R1)	2.96 \pm 0.88	2.90 \pm 0.91	3.40 \pm 0.85	3.50 \pm 0.96	3.24 \pm 0.97	3.67 \pm 0.94	4.25 \pm 0.85	3.90 \pm 0.97	3.65 \pm 0.83	3.27 \pm 0.86	0.59
Distal anastomosis (R2)	2.74 \pm 0.76	2.79 \pm 0.79	3.21 \pm 0.66	3.32 \pm 0.85	3.11 \pm 0.91	3.40 \pm 0.84	3.94 \pm 0.81	3.72 \pm 0.85	3.49 \pm 0.77	3.02 \pm 0.79	

was superior to all other temporal windows for visualization of distal anastomosis, irrespective of arterial or venous grafts, individual or sequential grafts, and the target coronary artery.

When using 16-slice CT, up to 23% of arterial and up to 8% of venous CABG segments were considered non-evaluative [14]. Moreover, 13–26% of the distal anastomoses had to be excluded from analysis [3, 5]. Major contributors to non-interpretability of CABG grafts are metallic clips and motion artifacts [2, 15]. Motion artifacts occur when the motion velocity of the structure of interest exceeds the temporal resolution of the CT scanner, particularly in patients with high heart rates. Thus, with former CT scanner generations individual selection of an appropriate temporal window for different CABGs was mandatory to reduce blurring artifacts [11, 15–17].

The proximal anastomoses and the body of venous CABGs are usually larger in size and show lower motion velocity compared with the coronary arteries; thus, visualization was successfully performed even with early CT scanners [18]. Consequently, the image quality of these segments was not significantly affected by the temporal window during cardiac cycle. In contrast, distal anastomoses are more prone to cardiac motion due to their close proximity to the coronary arteries. Thus, optimal temporal windowing more resembles that for the imaging of coronary arteries. With 16-slice CT, graft body and distal anastomosis to left anterior descending artery and left circumflex artery were best visualized at 60–70%, whereas the graft body and distal anastomosis to the right coronary artery was best visualized at 50% of the R-R interval [11]. Comparably, when using four-slice CT the temporal window had to be adapted to each coronary artery for optimal image quality [19]. The increased temporal and spatial resolution provided by the 64-slice CT scanner technique used in our study allowed best visualization of the distal anastomoses irrespective of the target coronary artery at 60% of the R-R interval. Interestingly, 64-slice CT provides diagnostic image quality in most temporal windows except at 0%, 10%, 40%, and 90% of the R-R interval. This might be explained by the coronary motion pattern, with rapid movement during ventricular contraction at early to mid-systole and during rapid filling in early diastole [20]. Moreover, our results demonstrate that 64-slice CT provides diagnostic visualization of all distal anastomoses. Therefore, our results are in line with recent publications analysing image quality of coronary artery segments at different temporal windows [9, 21–23]. These studies found the 60% R-R interval to be the best temporal window for all coronary artery segments. Moreover, a preliminary study on the assessment of CABG patency with 64-slice CT [10] reported that all CABGs and 94% of the distal anastomoses could be visualized. Reasons for non-evaluative visualization of distal anastomoses were clips or calcification-related artifacts and not motion artifacts in this study.

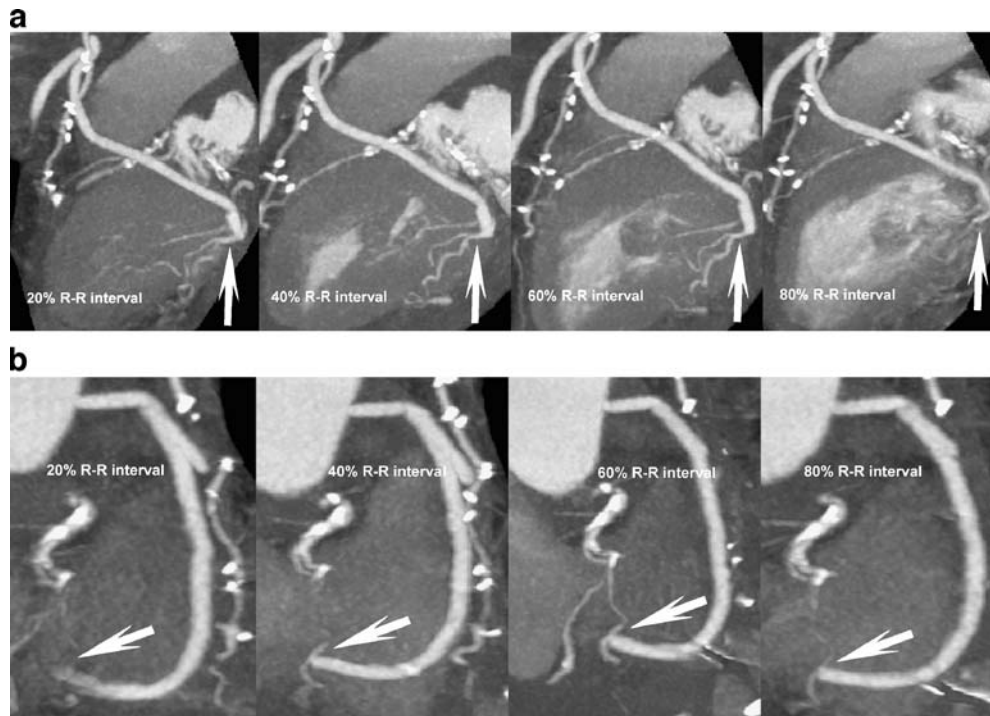


Fig. 3 A 77-year-old woman after CABG surgery with left internal mammary artery grafted to the left anterior descending artery (not shown) and saphenous vein graft in Y grafting technique to the posterior descending artery branch of the left circumflex artery and to the posterior lateral branch of the right coronary artery. **a** Maximum intensity projection of the distal anastomosis to the left circumflex artery (*arrow*) shows excellent image quality at 60% R-R

interval (score 5), while mild blurring renders good image quality at 20%, and 40% (score 4). Discontinuity and severe blurring at 80% leads to non-diagnostic image quality (score 1). **b** Maximum intensity projection of the distal anastomosis to the RCA (*arrow*) demonstrate good image quality at 40%, 60% and 80% of the R-R interval (score 5), but discontinuity at 20% (score 1) renders image quality non-diagnostic (score 1)

Most recently, dual-source CT have been introduced which further improved temporal resolution to 83 ms by simultaneously acquiring data with two X-ray tubes and two detectors mounted on the gantry with a 90° angular

offset (Flohr Eur Radiol). First experiences using dual-source CT reported its robustness of diagnostic image quality in a wide range of heart rates [24], and the high diagnostic accuracy for the assessment of coronary stenosis

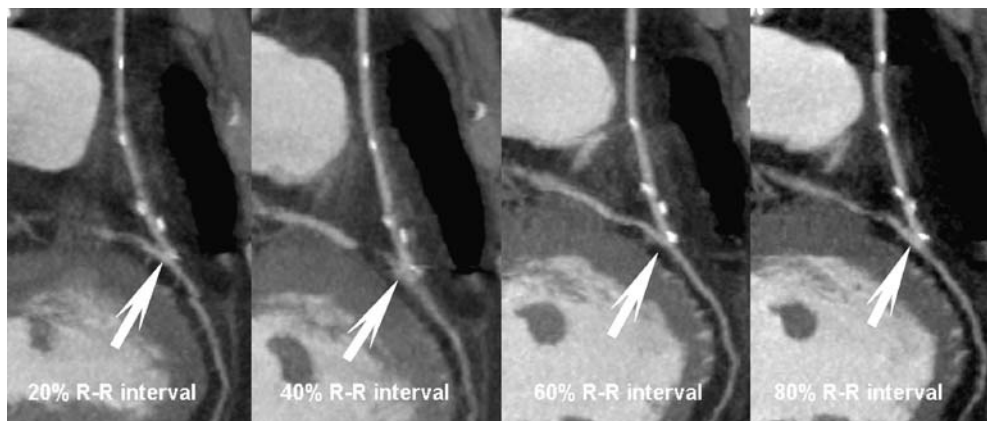


Fig. 4 A 59-year-old woman after CABG surgery with left internal mammary artery grafted to the middle segment of the left anterior descending artery. Maximum-intensity projection shows the arterial graft body with excellent image quality at 60% (score 5), good image quality (score 4) at 20% and 40%, and moderate (score 3) at 80%. Visualization of the distal anastomosis (*arrow*) is impaired at

20% and 40% of the R-R interval as a result of blurring artifacts occurred (score 2); at 60% the anastomosis outlines are sharply defined with only minimal clip artifacts hindering anastomosis visualization (score 4); at 80% mild blurring and irregularity of the vessel slightly impairs image quality (score 3)

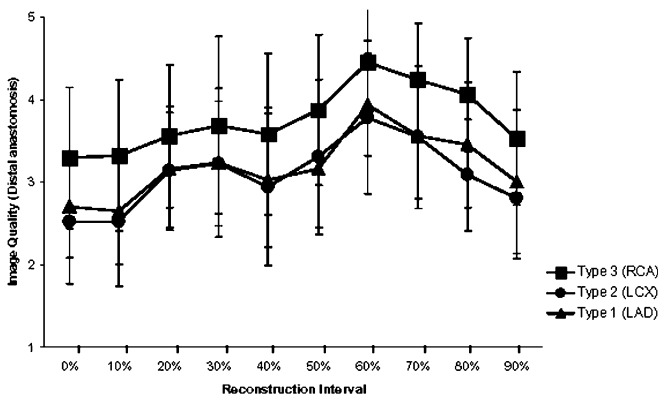


Fig. 5 Graph demonstrating the mean image quality of distal anastomosis in the evaluation of the three types of coronary artery bypass grafts: type 1, distal anastomosis to segments 6–10 (*LAD* left anterior descending artery); type 2, distal anastomosis to segments 11–15 (*LCX* left circumflex artery); and type 3, distal anastomosis to segments 1–4 (*RCA* right coronary artery). *Error bars* indicate \pm SD. Best image quality of distal anastomosis was obtained at 60% of the cardiac cycle in all types of grafts

without performing heart rate control by beta-blockers [25]. The application of dual-source CT might further improve the visualization of the distal anastomoses. In addition, dual-source CT will allow to narrow the full tube current window of ECG pulsing with a decrease of the slew rate. In combination with the adaptation of the pitch to the HR, the advanced tube current modulation may result in further radiation exposure savings.

CT coronary angiography is characterized by a substantial irradiation to the patient. CT for CABG imaging might lead to higher doses when including proximal anastomoses. For dose reduction in cardiac CT, the technique of ECG-controlled tube current modulation has been introduced [26]. This technique is characterized by a nominal tube output during mid- to end-diastole and a reduction of tube output to 20% during other parts of the cardiac cycle. The results of our study indicate that image reconstruction with 64-slice CT can be limited to a single time interval at 60%. This finding represents the rationale to implement the technique of ECG-pulsing in future CT studies for CABG imaging.

A major limitation of our study is that none of the patients underwent selective CABG angiography because examinations were performed for scientific purposes only. Therefore, we did not include assessment of bypass graft patency to prove our scoring threshold of diagnostic image quality. However, high diagnostic accuracy of 64-slice CT for assessment of CABG patency has been already shown [4]. Our primary study aim was to find the optimal timing for image reconstruction for different CABG segments and types and not to investigate the ability of CT to assess CABG patency. However, patients were highly pre-selected and the total number of 25 patients remains low considering the varied anatomy of CABGs; thus, transfer of our results to clinical practice might be limited. A second

limitation is the subjective nature of the image quality analysis. Nevertheless, the overall kappa value of 0.62 indicates a good inter-observer agreement and may argue against such a subjectivity bias. In addition, the ranking scale for image quality of CABG segments used merges artifacts derived from motion and metallic clips. Thus, lower image quality in arterial graft segments might be partly due to beam hardening artifacts. Third, images were reconstructed in 10% but not in 5% steps of the R-R interval. Fourth, 25 patients represent a rather small cohort that prevented a powerful subanalysis regarding the relationship of mean heart rate and heart rate variability on CABG image quality. Fifth, we focused our study on evaluating optimal temporal windows for CABG imaging. We did not compare image quality of the native coronary

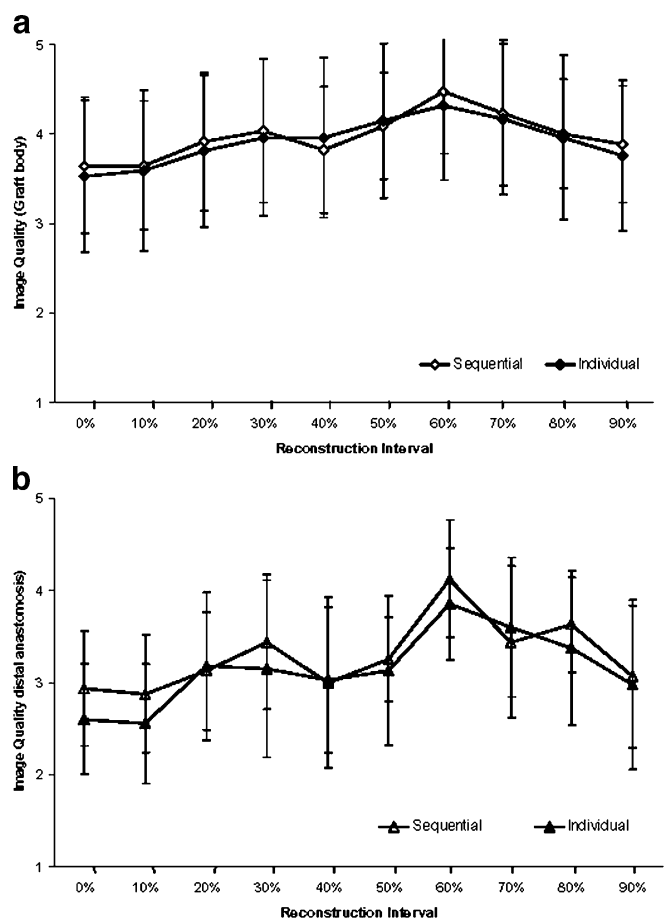


Fig. 6 Graphs demonstrating the mean image quality of graft body and distal anastomosis of sequential and individual grafts. *Error bars* indicate \pm SD. **a** Graphs of image quality in body segments indicate no significant difference between individual and sequential grafts (*P* value not significant), while image quality at 60% was significantly better compared with other temporal windows ($P < 0.001$). **b** Graphs of image quality in distal anastomosis demonstrate no significant difference between individual and sequential grafts (*P* value not significant). The temporal windows with best mean image quality for distal anastomosis was 60% for both individual and sequential grafts ($P < 0.001$)

arteries in different temporal windows in order to test if windows for CABG are also optimal for native coronary arteries. However, optimal reconstruction windowing has already been investigated in several previous studies, which constantly reported a mid-diastolic window superior to other temporal windows [9, 21–23]. In addition, patients who had undergone CABG surgery commonly present with severely calcified vessels which limit the impact of CT imaging of the native coronary arteries. Finally, we did not include evaluation of the subclavian arteries to visualize the proximal part of the internal mammary artery in order to reduce radiation exposure to the patient.

Conclusion

Sixty-four-slice CT angiography provides diagnostic image quality for all venous and 95% of all arterial CABG

segments. Image quality of proximal anastomoses does not depend on the temporal window, whereas distal anastomoses are visualized with best image quality at 60% of the R-R-interval, irrespective of arterial or venous graft, the target coronary artery, and individual or sequential grafts. Thus, data reconstruction with 64-slice CT for evaluating CABG can be initially restricted to a single temporal window during mid-diastole, which provides the rationale to implement the ECG-pulsing technique to reduce the radiation dose applied to the patient.

Acknowledgements This research has been supported by the National Center of Competence in Research, Computer Aided and Image Guided Medical Interventions of the Swiss National Science Foundation.

References

1. Yoo KJ, Choi D, Choi BW, Lim SH, Chang BC (2003) The comparison of the graft patency after coronary artery bypass grafting using coronary angiography and multi-slice computed tomography. *Eur J Cardiothorac Surg* 24:86–91; discussion 91
2. Marano R, Storto ML, Maddestra N, Bonomo L (2004) Non-invasive assessment of coronary artery bypass graft with retrospectively ECG-gated four-row multi-detector spiral computed tomography. *Eur Radiol* 14:1353–1362
3. Schlosser T, Konorza T, Hunold P, Kuhl H, Schmermund A, Barkhausen J (2004) Noninvasive visualization of coronary artery bypass grafts using 16-detector row computed tomography. *J Am Coll Cardiol* 44:1224–1229
4. Pache G et al (2006) Initial experience with 64-slice cardiac CT: non-invasive visualization of coronary artery bypass grafts. *Eur Heart J* 27:976–980
5. Anders K et al (2006) Coronary artery bypass graft (CABG) patency: assessment with high-resolution submillimeter 16-slice multidetector-row computed tomography (MDCT) versus coronary angiography. *Eur J Radiol* 57:336–344
6. Khan MF et al (2005) Visualisation of non-invasive coronary bypass imaging: 4-row vs. 16-row multidetector computed tomography. *Eur Radiol* 15:118–126
7. Yamamoto M, Kimura F, Niinami H, Suda Y, Ueno E, Takeuchi Y (2006) Noninvasive assessment of off-pump coronary artery bypass surgery by 16-channel multidetector-row computed tomography. *Ann Thorac Surg* 81:820–827
8. Flohr T, Stierstorfer K, Raupach R, Ulzheimer S, Bruder H (2004) Performance evaluation of a 64-slice CT system with z-flying focal spot. *Rofo* 176:1803–1810
9. Leschka S et al (2006) Optimal image reconstruction intervals for non-invasive coronary angiography with 64-slice CT. *Eur Radiol* 16:1964–1972
10. Malagutti P et al (2006) Use of 64-slice CT in symptomatic patients after coronary bypass surgery: evaluation of grafts and coronary arteries. *Eur Heart J*
11. Willmann JK et al (2004) Coronary artery bypass grafts: ECG-gated multidetector row CT angiography-influence of image reconstruction interval on graft visibility. *Radiology* 232:568–577
12. Austen WG et al (1975) A reporting system on patients evaluated for coronary artery disease. Report of the Ad Hoc Committee for Grading of Coronary Artery Disease, Council on Cardiovascular Surgery, American Heart Association. *Circulation* 51:5–40
13. Alkadhi H et al (2005) Dynamic cine imaging of the mitral valve with 16-MDCT: a feasibility study. *AJR Am J Roentgenol* 185:636–646
14. Stauder NI et al (2006) Coronary artery bypass grafts: assessment of graft patency and native coronary artery lesions using 16-slice MDCT. *Eur Radiol* 16:2512–2520
15. Nieman K, Pattynama PM, Rensing BJ, Van Geuns RJ, De Feyter PJ (2003) Evaluation of patients after coronary artery bypass surgery: CT angiographic assessment of grafts and coronary arteries. *Radiology* 229:749–756
16. Burgstahler C et al (2003) Non-invasive evaluation of coronary artery bypass grafts using multi-slice computed tomography: initial clinical experience. *Int J Cardiol* 90:275–280
17. Ropers D et al (2001) Investigation of aortocoronary artery bypass grafts by multislice spiral computed tomography with electrocardiographic-gated image reconstruction. *Am J Cardiol* 88:792–795
18. Brundage BH et al (1980) Detection of patent coronary bypass grafts by computed tomography. A preliminary report. *Circulation* 61:826–831
19. Kopp AF et al (2001) Coronary arteries: retrospectively ECG-gated multidetector row CT angiography with selective optimization of the image reconstruction window. *Radiology* 221:683–688
20. Lu B et al (2001) Coronary artery motion during the cardiac cycle and optimal ECG triggering for coronary artery imaging. *Invest Radiol* 36:250–256
21. Bley TA et al (2005) Computed tomography coronary angiography with 370-millisecond gantry rotation time: evaluation of the best image reconstruction interval. *J Comput Assist Tomogr* 29:1–5

22. Frydrychowicz A et al (2007) Comparison of reconstruction intervals in routine ECG-pulsed 64-row-MSCT coronary angiography in frequency controlled patients. *Cardiovasc Intervent Radiol* 30:79–84
23. Wintersperger BJ et al (2006) Image quality, motion artifacts, and reconstruction timing of 64-slice coronary computed tomography angiography with 0.33-second rotation speed. *Invest Radiol* 41:436–442
24. Johnson TR et al (2006) Dual-source CT cardiac imaging: initial experience. *Eur Radiol* 16:1409–1415
25. Scheffel H et al (2006) Accuracy of dual-source CT coronary angiography: First experience in a high pre-test probability population without heart rate control. *Eur Radiol* 16:2739–2747
26. Jakobs TF et al (2002) Multislice helical CT of the heart with retrospective ECG gating: reduction of radiation exposure by ECG-controlled tube current modulation. *Eur Radiol* 12:1081–1086